The SEMAPHORO Haptic Interface: a real-time low-cost open-source implementation for dyadic teleoperation

Lucas Roche, Florian Richer, Ludovic Saint-Bauzel

The SEMAPHORO* Haptic Interface: a real-time low-cost open-source implementation for dyadic teleoperation

Lucas Roche[1], Florian Richer[1] and Ludovic Saint-Bauzel[1]

Abstract—In this paper, a one degree of freedom teleoperation interface is presented. The design of this device focuses on realizing a low-cost controller able to obtain good real-time performances for the acquisition of physical data during the interaction. Design choices and hardware used are presented, as well as the control strategy used for attaining transparency in teleoperation. The controller is able to maintain a 5kHz frequency control for the teleoperation, running on a BeagleBone black motherboard. The performances of the interface are presented and analyzed.

1 Introduction

The need of advanced robotics in industrial fields is increasing. Classical industrial robots are progressively replaced by cobots and robots that share their workspace with humans. This implies the ability for robotic devices to be safely manipulated and remotely or in contact, since users may have to participate to the robot operation. Such features require to provide haptic feedback to the remote operator, which is possible using bilateral teleoperation control schemes. Bilateral teleoperation is increasingly used in a wide range of industrial applications, varying from operation in hazardous environment to micro-assembly, or control of mobile robots [1] [2] [3]. In the case where the robot is in contact with two operators, the controller needs to share the information to each actor of the system. Shared control of a robot by two humans will be called dyadic teleoperation in this paper.

In this configuration, the two users each control one manipulator, and a teleoperation controller ensures a transfer of forces and positions, so that a sense of physical interaction is recreated remotely. While not commonly used in the industrial world, dyadic teleoperation has multiple potential applications: shared manipulation with an expert has been proven to improve learning [4][5], and could be used to create efficient training in complex visuo-motor tasks, such as precise assembly. Shared control of robotized manipulator is also a growing trend in industrial context, where humans are getting back to the assembly lines.

Research on the topic of physical Human-Human Interaction and haptic communication has already proven that haptic feedback has a great influence on the success of dyadic comanipulation between humans. It has been shown to convey emotions [6] as well as an increased sense of telepresence [7] [8]. It also allows for better learning [9] [8] and performances in tracking tasks, even in cases of conflict [10]. In conclusion, many studies point at the haptic channel as an efficient mean of communication between humans [11] [12] [13] [14] [10].

If the existence of this haptic communication ability in human dyads is a well accepted theory, the understanding of the mechanisms behind it is still lacking to this day. Groten & al. [10] linked haptic communication to the energy exchanges inside the dyad, in order for the partners to negotiate between their individual motion plans. Tagaki & al. [5] advance that the Central Nervous System can interpret the force signals from the haptic link and recreate the motion plan of their partner.

These progresses in the study of pHHI towards efficient dyadic teleoperation rely on the use of high performing and precise teleoperation interfaces. The design of those devices, especially for industrial applications, requires to balance two main constraints: stability and performance. The stability of the system is of great importance in order to guarantee the safety of the users and the device. Performance on the other hand is essential for the efficiency of the teleoperation, and the comfort of the user. These two aspects are generally antagonist and practical teleoperation systems are as result generally expensive and/or complex and oversized. This expensive design is also a reason of the reduced amount of industrial applications.

The objective of this paper is to present a proof of concept implementation of a robust and high performing bilateral teleoperation setup on an open-source DIY interface. Focus is made on the use of low-cost and easily available components. The interface presented here has one degree of freedom, but the same core design can be expended up to three degrees of freedom with the same hardware. This demonstrative setup could be useful to research teams or start-ups wanting to experiment with haptic interfaces and pHHI without investing in a complex commercial solution.

All details of the interface are open-source and can be found at [15].

2 Design and technical details

2.1 Actuation

In order to reduce the potential friction and backlash in the system, the interface is designed with a direct drive

*Système d'Évaluation de la MAnipulation Physique HOmme-RObot - System for the Evaluation of Human-Robot Physical Manipulation

[1]Institut des Systèmes Intelligents et de Robotique, Université Pierre et Marie Curie, 75005 Paris, France roche@isir.upmc.fr saintbauzel@isir.upmc.fr

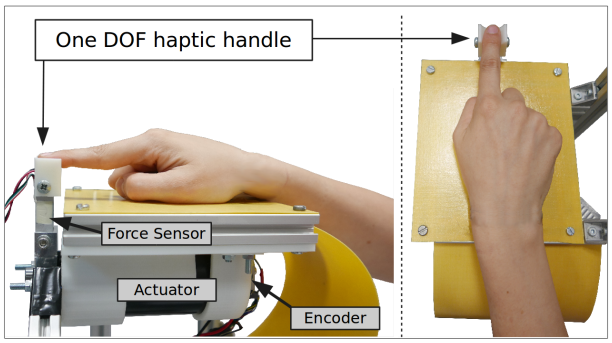

Fig. 1: The SEMAPHORO interface. A one degree-of-freedom haptic interface conceived for lightweighted and precise bilateral teleoperation.

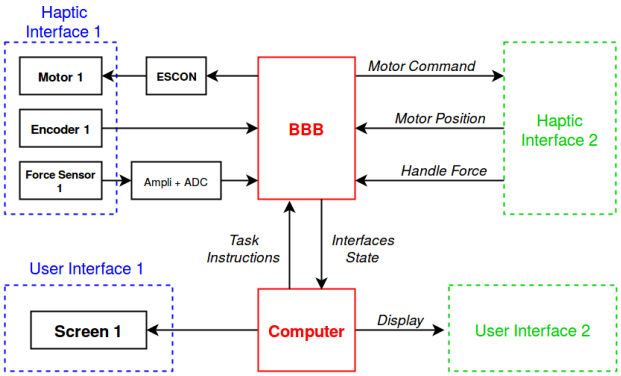

Fig. 2: Architecture and data flow of the robot hardware.

actuation. The only impedance introduced thus comes from the motor, and the mechanical inertia of the handle. The main drawback of direct drive actuation is the need for more powerful motors to be able to generate a sufficient torque in the absence of reductor. The designed interfaces uses two MAXON DC Motors (RE65-250W), connected to a 80mm handle. A schematic model of the haptic handle is represented in Figure 1.

2.2 Sensors

A magnetic encoder (CUI INC AMT11) is assembled to the motor shaft. The encoder precision is 4096 point per rotation, which translate to a minimal measurable displacement of the handle of 0.035 mm. Since the interface is in direct drive, there is no reduction of the motor motion, and it is necessary to use high precision position sensors to ensure the quality of the position control.

The force applied to the handle is measured with a load cell assembled in the handle's body. The use of a load cell (1DoF sensor) is sufficient in our application since only the torque applied around the motor axis is of interest. This torque is directly proportional to the tangential force applied to the handle, which we measure here with a from-the-shelf load cell. The use of the load cell is further justified by its reduced cost and ease of integration compared to a torque sensor. The load cells used can measure forces in the range [-50N; 50N], and have an inherent precision of 0.05N. The data is sampled by an 12 bits ADC, which precision is greater than the sensor's one.

An additional sensor is used as a form of security in the interfaces control: small conductive plates are positioned on the tip of the handles, and are connected to an open circuit voltage divider. When a finger comes in contact to the plates, it closes the circuit and a rise in voltage is measured. This is used to adjust the controller in presence or not of human contact.

2.3 Hardware

The controller is installed on a BeagleBone Black ARM development board (BBB) running a Xenomai Real-Time Operating System. The motors are interfaced with the controller through Maxon ESCON controllers, driven in current control by PWM inputs generated on the BBB. The encoders signals are monitored via the eqep modules of the BBB.

The acquisition cards available with most load cells sold do not reach acquisition frequencies compatible with real-time control. A custom made acquisition cards is thus used to amplify and convert the analog signals from the load cells. This acquisition card uses TI INA125 amplificators and a Maxim MAX1247 12 bits ADC.

The controller is connected to a second computer used to generate virtual scenarios based on the sensory inputs of the interfaces (position and force). The connection is ensured by TCP network through a direct Ethernet link, introducing a latency of less than 50 μs. The data acquisition as well as the control of the motor is realized at a 2kHz frequency. Communication with the User Interface is realized at 100 Hz (adjustable according to the needs). Data recording is sampled at 2 kHz.

Figure 2 summarizes the hardware architecture and data flows between the different parts of the robot.

3 Control

The principal objective of teleoperation controllers is to reproduce a rigid link between the master manipulator (held by the user) and the slave manipulator (in contact with the environment). The ideal telemanipulator would consist in a stick of zero mass and infinite stiffness, allowing to transfer the distant environment impedance to the user perfectly. The quality of this impedance transfer is generally called *transparency*, and is the principal criterion when comparing two teleoperators. In pHHI applications, both manipulators have similar roles and are in contact with users. In this configuration, obtaining excellent transparency allows to ensure that both users can accurately feel the displacements and forces applied by their partner.

The second objective of teleoperation controllers is to ensure the stability of the system, in order to guarantee the safety of the users, the environment and the robot. Combining stability and transparency in teleoperation is however a tedious problem [16] [17] [18]. Multiple teleoperation controllers have been proposed since the first telemanipulators were conceived. A good review of literature on teleoperation can be found in [19].

3.1 Position-Position Control

Historically, the first solution used in teleoperation was to implement Position-Position (PP) control. In PP control, each interface is controlled with a PD controller targeting the position of the other interface. The force command of each interface is therefore expressed as:

$$F_{c,i} = K_P(x_{1-i} - x_i) + K_D(\dot{x_{1-i}} - \dot{x_i}) \quad (1)$$

with $i \in (0,1)$ designing the interface number, $F_{c,i}$ the force command for the interface i, x_i its position, and $\dot{x_i}$ its velocity.

The result of this controller is a spring-damper-like link between the two interfaces, which characteristics can be controlled by tuning K_P (stiffness) and K_D (damping). The biggest advantage of the PP controller is its simplicity : its implementation only requires position sensors, and its stability can be guaranteed for a range of gain values.

Implementations of PP control however have severe limitations on maximal stiffness rendered while stable, especially for lighter manipulators. Better control strategies have since been developed which are generally preferred in teleoperation applications. It is however still used in most pHHI research setups for its simplicity.

3.2 Admittance control

Admittance control, introduced by Hogan [20], can be used to create a stiff link between the interfaces in pHHI setups. In admittance control, the forces applied to the interfaces are used as an input for a modelization of a virtual object of known impedance. The displacements of the virtual object produced by the applied forces are then reproduced as an output by the interfaces. The resulting control is equivalent to a virtual mass connected to both controllers by a spring/damper link. Admittance control allows to precisely tune the impedance characteristics wanted for the interface. However, to guarantee stability in impedance control, there is a limit on the mass/impedance ratio that can be rendered [17]. In the case of lightweighted tasks, where the apparent mass of the haptic interface must be kept as low as possible, the range of possible stiffness rendered is generally limited. Moreover, in most dyadic teleoperation scenarii, it is preferable to compensate for the interfaces impedance, which is not possible in admittance control. Admittance control is used in multiple research setups in the literature, but is not fit for the applications presented in the scope of this paper, and will thus not be considered further.

3.3 Control theory for teleoperation

Control theory in teleoperation was refined in the early 90's and allowed to obtain better transparency than PP control.

A teleoperated system can be represented by an hybrid matrix H(s) defined as:

$$\begin{bmatrix} F_1 \\ -V_2 \end{bmatrix} = H(s) \begin{bmatrix} V_1 \\ F_2 \end{bmatrix} = \begin{bmatrix} h_{11} & h_{12} \\ h_{21} & h_{22} \end{bmatrix} \begin{bmatrix} V_1 \\ F_2 \end{bmatrix} \quad (2)$$

Using the hybrid matrix of the teleoperated system and the definnition of the task impedance $Z_e = \frac{F_e}{V_e}$ we can express the impedance "felt" by the operator as

$$Z_t = \frac{F_h}{V_h} = \frac{h_{11}(1 + h_{22}Z_e) - h_{21}h_{12}Z_e}{1 + h_{22}Z_e} \quad (3)$$

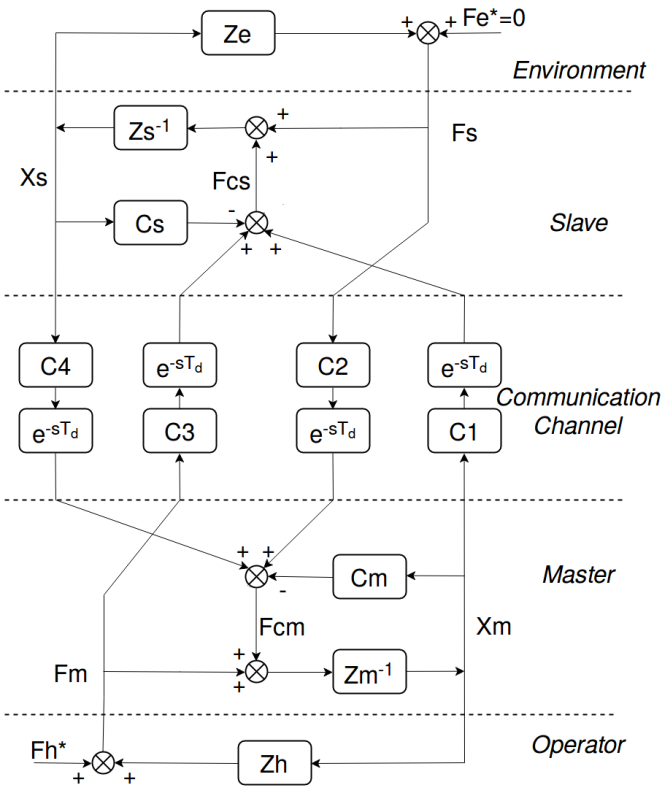

Fig. 3: Four Channel Architecture as described by Lawrence.

.

Ideal transparency is defined as perfect transmission of environment impedance to the master : $Z_t = Z_e$, thus, we can deduce from (3) the necessary and sufficient condition for transparency:

$$\begin{aligned} h_{11} = h_{22} = 0 \\ h_{12}h_{12} = -1 \end{aligned} \quad (4)$$

3.4 The Four Channels Architecture

Lawrence[16] and Yokokohji[21] published work on transparency including a theoretical analysis of the teleoperation problem, and realized that perfect transparency can be obtained if both force and position signals are used for the control of both master and slave manipulators. The controller strategy they proposed, called Four Channel (4C) Architecture, is still considered the simplest implementation of a control architecture allowing theoretical perfect transparency in teleoperation. It has been proven to offer the best performances amongst the usual teleoperation schemes [22].

The 4C architecture is presented in Figure 3.

Expressing the transmitted impedance in terms of the block transfer functions leads to :

$$Z_t = \frac{[(Z_m + C_m)(Z_s + C_s) + C_1C_4] + Z_e(Z_m + C_m + C_1C_2)}{(Z_s + C_s - C_3C_4) + Z_e(1 - C_2C_3)} \quad (5)$$

This architecture allows perfect transmission of impedance from slave to master and from master to slave for the following set of controllers :

$$\begin{array}{ll} C_m = K_P + K_D s & C_s = K_P + K_D s \\ C_1 = C_s + Z_s & C_2 = 1 \\ C_3 = 1 & C_4 = C_m + Z_m \end{array}$$

Perfect transparency however requires to include the master and slave impedances in the controllers. These values are only possible to compute accurately with a good measure of the acceleration. Without accelerometers on the system, this value must be obtained by a double derivative of the position measure, which is certain to introduce a lot of noise in the system. Zhu & Salcudean [23] proposed a variation of the perfectly transparent four channels obtained with the following controllers:

$$\begin{array}{ll} C_m = K_P + K_D s & C_s = K_P + K_D s \\ C_1 = C_s & C_2 = 1 \\ C_3 = 1 & C_4 = C_m \end{array}$$

Which allows to have perfect transmission of position, while keeping $Z_t = Z_e + Z_m$, effectively keeping only the master's impedance felt by the user in addition to the environment impedance. In our application, the master's impedance is low enough (cf Part 4.2) for this solution to be acceptable, which avoid the use of accelerometers or double derivative. Moreover, it may be better in certain applications to keep an apparent impedance [24].

3.5 Gain adaptation between free and constrained motion

Performance in constrained mode, especially for high environment impedance, is enhanced by increasing the position control gain values: the higher the better. However, higher gains values tend to deteriorate the stability in free mode. In order to compromise with these two contradictory constraints, the control of the interface includes gain scheduling as way to react to environment impedance changes adaptively. The gains K_P and K_D (gains are the same for master ad slave controllers) are calculated with the following formula:

$$\begin{array}{c} K_x = K_{x_{min}} + \dfrac{F_{int}}{F_{int_{MAX}}} K_{x_{MAX}} \\ with\ x = \{P, D\}\ \ and\ F_{int} = |F_1 - F_2| \end{array} \quad (6)$$

$K_{x_{min}}$ are chosen as the maximal gains allowing for stability in free mode, $K_{x_{MAX}}$ are tuned for stability in constrained mode, and to increase the performance while guarantying that the system's power limits are not reached during the task. $F_{int_{MAX}}$ is tuned according to the specific task (in our case, it was estimated that the interaction force between the subjects would not exceed 24N). The gain adaptation can also be used to enhance performances when force data acquisition frequency is low, or when there is a discrepancy between the acquisition frequencies and loop frequencies.

The implemented teleoperation scheme is described in Fig 4. The gains are chosen as :

$$\begin{array}{ll} C_m = K_P + K_D s & C_2 = 1 \\ K_{P_{min}} = 400 & K_{P_{MAX}} = 1000 \\ K_{D_{min}} = 2 & K_{D_{MAX}} = 5 \end{array}$$

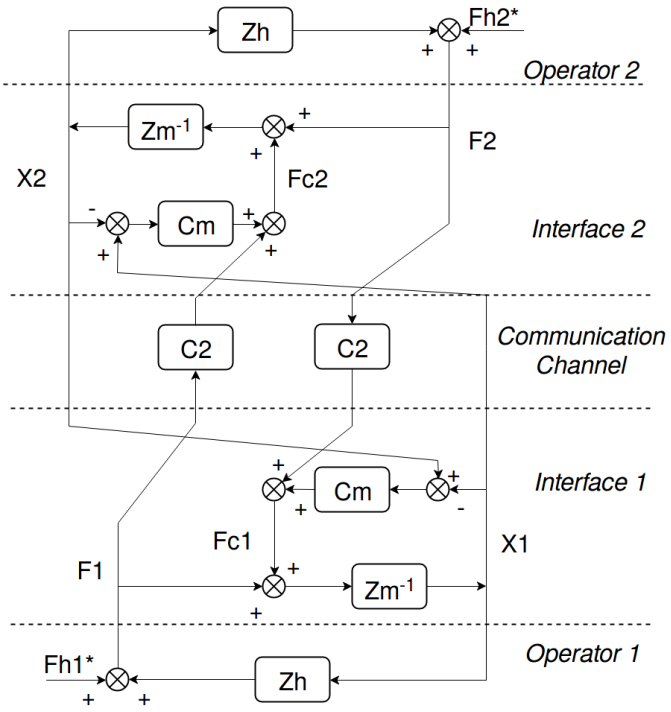

Fig. 4: Variation of the Four Channel Architecture implemented in the interface.

3.6 Symmetry of the set-up

Most of the literature about teleoperation control addresses the case of a human manipulating the master interface, to interact with a passive environment on the slave side. In our application, both the slave and master sides are in contact with an active human operator. Symmetry of both the interfaces and control are here essential. The four channels architecture allows perfect symmetry of the transmitted impedances on master and slave sides: with the block controllers presented earlier, the transmitted impedance on master side is $Z_t = Z_e + Z_m$, symmetrically, from the slave's point of view, the transmitted impedance is $Z_{end} = Z_m + Z_h$ which guaranties equality of the transmitted impedances as long as $Z_m = Z_s$, which is ensured by the mechanical design of the interfaces.

4 System Characterization

The inertia and friction of the interfaces are characterized to ensure they are low enough not to influence the behavior of the controller and the transmitted impedance. Indeed, the teleoperation control presented earlier reaches optimal performances for low inertia interfaces, and internal friction is not accounted for in the model.

4.1 Torque response

In order to evaluate the motor open-loop frequency response for torque generation, the haptic interfaces were blocked isometrically, so that the force sensors only measured the efforts coming from the actuation. A sine sweep

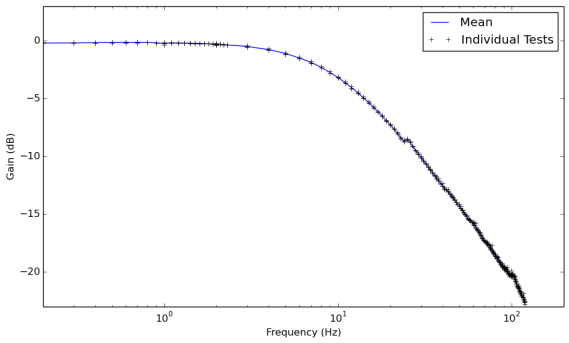

Fig. 5: Amplitude of the open-loop frequency response of the interface. The response was obtained with a sine sweep method. Individual tests for each frequencies are displayed, as well as the average corresponding curve.

method was then employed to study the response of the system. The excitation signal was in the form of:

$$I_{excitation} = A_e \sin(2\pi f_k t) \tag{7}$$

With f_k the frequency of the signal varying from 0.2 Hz to 120 Hz (increments were 0.1 Hz until 2 Hz, and 1 Hz after). The amplitude A_e of the signal was calculated to generate a 5 N force amplitude on the handle.

$$A_e = \frac{F_e.L_h}{K_m} = \frac{5 \times 0.08}{0.123} = 3.25A \tag{8}$$

With F_e the target force of 5 N, L_h the distance between the motor axis and the handle fixation, and K_m the motor torque constant.

Each frequency was tested for 5 periods, on three repetitions. The force response of the signal was recorded and compared to the theoretical force expected according to the excitation. The amplitude of the frequency response is shown in Figure 5. The system behaves approximatively as a first order low-pass, with a flat response before 8 Hz, then a fall for the higher frequencies. The bandwith of the system is 10 Hz, defined with a cutoff at -3 dB. This bandwith is quite limited to render the full range of human sensorimotor capacities, which partly relies on higher frequencies [25]. It is although sufficient to render the full range of human voluntary motions, which frequencies do not exceed 10 Hz [25].

4.2 System parameters analysis

The haptic interface without human effort input can be modeled as a simple rigid mass with one degree of freedom in rotation around the motor axis. Considering the motor as sole source of external effort, the dynamic equation of the system can be written as:

$$J_h.\ddot{\theta} = \tau_m - \tau_f \tag{9}$$

where J_h represents the total inertia of the handle, θ the angular position of the handle around the motor axis, τ_m the motor torque and τ_f is expressed as:

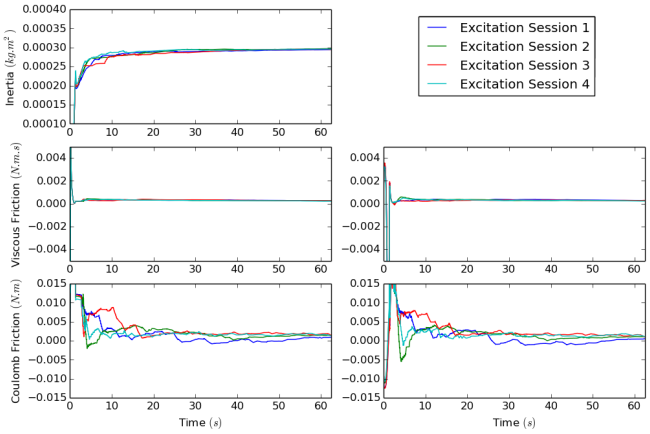

Fig. 6: Offline convergence of the system's dynamic parameters estimation using RLS over four excitation sessions of 60 s.

$$\tau_f = \begin{cases} \beta_1\dot{\theta} + \beta_3 sign(\dot{\theta}) & sign(\dot{\theta}) > 0 \\ \beta_2\dot{\theta} + \beta_4 sign(\dot{\theta}) & sign(\dot{\theta}) < 0 \\ 0 & \dot{\theta} = 0 \end{cases} \tag{10}$$

where β_1 and β_2 are the viscous friction coefficients and β_3 and β_4 are the Coulomb friction coefficients [26].

This dynamic equation can be expressed linearly as :

$$\begin{aligned} \tau_m = J_h\ddot{\theta} + \beta_1\dot{\theta}F(\dot{\theta}) + \beta_2\dot{\theta}F(-\dot{\theta}) \\ + \beta_3 sign(\dot{\theta})F(\dot{\theta}) + \beta_4 sign(\dot{\theta})F(-\dot{\theta}) \end{aligned} \tag{11}$$

with:

$$F(\dot{\theta}) = \begin{cases} 1 & sign(\dot{\theta}) > 0 \\ 0 & else \end{cases} \tag{12}$$

In order to identify the unknown system parameters $(J_h, \beta_{1,2,3,4})$, the system is excited in free mode with a pseudo-randomly generated signal during four sessions, each lasting 60 seconds. The signal used as a bounded frequency spectrum, which is relatively flat for the 0.1 Hz - 10 Hz range; see [26] for the equations of the signal.

Offline Recursive Least Square (RLS) was used in order to estimate the parameters. The convergence of the parameters is shown in Figure 6. The average values over the sessions in used as final estimated values for the parameters : $J_h = 2.96\times10^{-4} kg.m^2, \beta_1 = 2.40\times10^{-4} N.m.s, \beta_2 = 2.61\times10^{-4} N.m.s, \beta_3 = 1.25 \times 10^{-3} N.m, \beta_4 = 0.918 \times 10^{-3} N.m.$ The system shows low values of inertia and friction, which are compatible with the teleoperation controller described earlier.

5 Evaluation of the Interface's Performances

5.1 Real-Time performance

Precision and reliability of the real-time loop of the controller are important characteristics in order to attain optimal performances of the haptic interface. In order to test

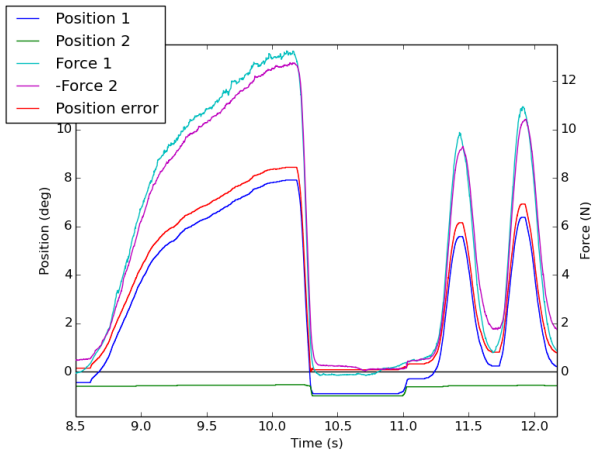

(a) Example trajectories and forces in constrained motion with PP control.

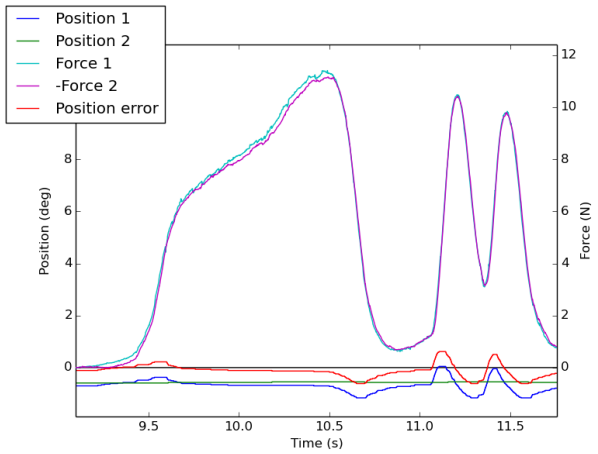

(b) Example trajectories and forces in constrained motion with 4C control.

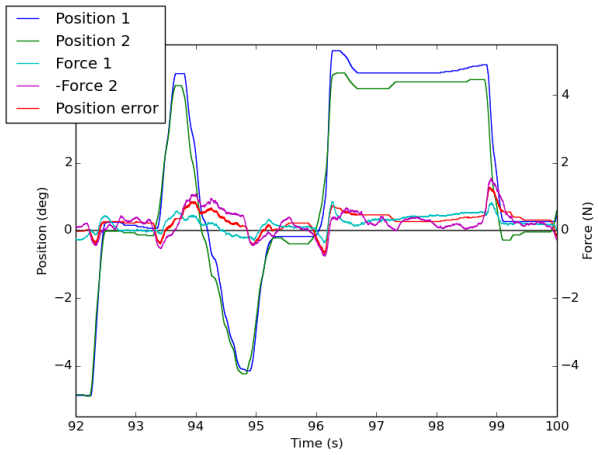

(c) Example trajectories and forces in free motion with PP control.

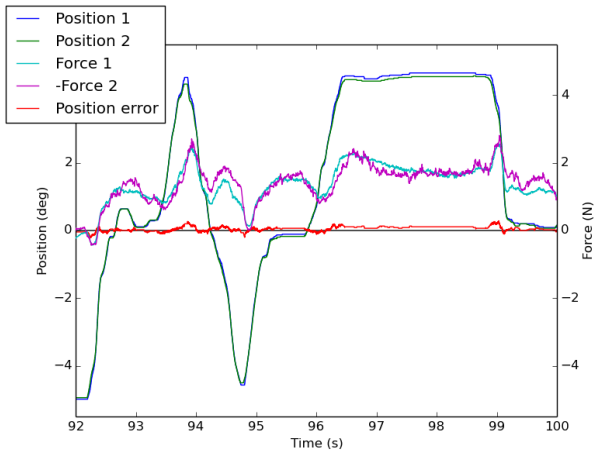

(d) Example trajectories and forces in free motion with 4C control.

the robustness of the implemented controller, various demanding tasks are executed and the loop time execution is recorded. The tasks are akin to those performed during actual usage of the interface (data sampling, motors control, data exchange with the graphical interface...). A total of 5 minutes of recording is analyzed. The target frequency of the loop is 5 kHz. 97.28% of the loops recorded were within 1% error of the target period (i.e between 0.198ms and 0.202ms). 98.27% of the loops were executed between 0.190ms and 0.210ms (less than 5% error), and 99.89% with less than 10% error from the target.

5.2 Control Scheme performances

Performances of a teleoperation interface can be measured in multiple ways, including: position tracking in free mode (measure of h_{12}), force tracking in constrained mode (measure of h_{21}), force/velocity relationship in free mode (measured of apparent master impedance). The performances of teleoperated interfaces are generally worse in rigidly constrained mode, i.e when one extremity in immobilized by contact with an infinitely rigid environment.

Figure 7a illustrates the trajectories of and forces applied to the interfaces when controlled with a Position-Position Controller in constrained motion against a rigid obstacle (with gains $K_P = 500$, $K_D = 3$). The mean force error between $|F_1|$ and $|F_2|$ during the test is 0.44 N, corresponding to an average 8.5% relative force error. The average position error is 3.4° (4.8 mm at the end effector).

Figure 7b shows the same parameters for interfaces controlled with a 4C Architecture. The mean force error between $|F_1|$ and $|F_2|$ during the test is 0.14 N, corresponding to an average 3.5% relative force error. The average position error is 0.25° (0.35 mm at the end effector).

Tests trajectories in free mode are done by human participants. Average position error was 0.27° (0.37 mm) for the PP controller, and 0.045° (0.066 mm) for the 4C controller.

The maximal stiffness rendered by the interface in actual use is measured to reach $2 \times 10^4 N.m^{-1}$. The minimal stiffness required to experience the sensation of hardness have been proposed to be around $10^4 N.m^{-1}$ [27] [28] [25]. The performance of the proposed interface should thus be sufficient to simulate a rigid connection between the two handles.

The proposed controller architecture allows for a significant increase in performances compared to a traditional teleoperation controller. The overall performances of the interface are validated for use in human-human studies on

haptic interaction.

6 Conclusion

This paper presented an implementation of a teleoperation controller for a dual haptic interface. The controller is designed to operate on low-cost hardware, while still keeping good performances: the control loop operates at 5 kHz (2 kHz for the force acquisition, limited by the I2C protocol). The device is able to provide very accurate position and force tracking and is suited for studies on human-human comanipulation. All details of the interface are open-source and can be found at [15].

References

[1] S. Lichiardopol, "A survey on teleoperation," *Technische Universiteit Eindhoven - DCT report*, 2007.

[2] R. Boboc, H. Moga, and D. Talaba, "A review of current applications in teleoperation of mobile robots," *Bulletin of the Transilvania University of BraÅŞov*, 2012.

[3] A. Bolopion and S. RÃľgnier, "A review of haptic feedback teleoperation systems for micromanipulation and microassembly," *IEEE Transactions on Automation Science and Engineering*, 2013.

[4] S. Jacobs, D. Holzhey, G. Strauss, O. Burgert, and V. Falk, "The impact of haptic learning in telemanipulator-assisted surgery," *Surgical Laparoscopy, Endoscopy and Percutaneous Techniques Percutaneous Techniques*, 2007.

[5] A. Takagi, G. Ganesh, T. Yoshioka, M. Kawato, and E. Burdet, "Physically interacting individuals estimate the partnerâĂŹs goal to enhance their movements," in *Nature Human Behavior*, 2017.

[6] J. N. Bailenson, N. Yee, S. Brave, D. Merget, and D. Koslow, "Virtual interpersonal touch: Expressing and recognizing emotions through haptic devices," *Human-Computer Interaction*, vol. 22, pp. 325–353, 2007.

[7] C. Basdogan, C. Ho, M. A. Srinivasan, and M. Slater, "An experimental study on the role of touch in shared virtual environments," *ACM Transactions on Computer-Human Interaction*, vol. 7, no. 4, pp. 443–460, 2000.

[8] A. Chellali, C. Dumas, and I. Milleville-Pennel, "Influence of haptic communication on a shared manual task in a collaborative virtual environment," *Interacting with Computers*, 2011.

[9] G. Ganesh, A. Tagaki, T. Yoshioka, M. Kawato, and E. Burdet, "Two is better than one: Physical interactions improve motor performance in humans," *Nature, Scientific Report 4:3824*, 2014.

[10] R. Groten, D. Feth, R. L. Klatzky, and A. Peer, "The role of haptic feedback for the integration of intentions in shared task execution," *IEEE Transactions on Haptics, Vol 6, No 1*, 2013.

[11] J. Moll and E.-L. Sallnas, "Communicative functions of haptic feedback," *Haptic and Audio Interaction Design*, 2009.

[12] A. Sawers, T. Bhattacharjee, J. L. McKay, M. E. Hackney, C. C. Kemp, and L. H. Ting, "Small forces that differ with prior motor experience can communicate movement goals during human-human physical interaction," *Journal of NeuroEngineering and Rehabilitation*, 2017.

[13] R. P. V. der Wel, G. Knoblitch, and N. Sebanz, "Let the force be with us: Dyads exploit haptic coupling for coordination," in *Journal of Experimental Psychology: Human Perception and Performance*, 2010.

[14] C. A. C. Parker and E. A. Croft, "Experimental investigation of human-robot cooperative carrying," *IEEE/RSJ International Conference on Intelligent Robots and Systems*, 2011.

[15] L. Roche and L. Saint-Bauzel, "teleop-controller-bbb-xeno : https://github.com/ludovicsaintbauzel/teleop-controller-bbb-xeno," 2017.

[16] D. A. Lawrence, "Stability and transparency in bilateral teleoperation," *IEEE Transactions on Robotics and Automation. vol. 9, no. 5*, 1993.

[17] J. E. Colgate and J. M. Brown, "Factors affecting the z-width of a haptic display," in *Proceedings of the 1994 IEEE International Conference on Robotics and Automation*, 1994.

[18] D. W. Weir and J. E. Colgate, *Stability of Haptic Displays*, ch. 8. CRC Press, 2009.

[19] P. F. Hokayem and M. W. Spong, "Bilateral teleoperation: A survey," *Automatica 42*, 2006.

[20] N. Hogan, "Impedance control - an approach to manipulation.," *ASME Transactions Journal of Dynamic Systems and Measurement Control B*, vol. 107, pp. 1–24, Mar. 1985.

[21] Y. Yokokohji and T. Yoshikawa, "Bilateral control of master-slave manipulators for ideal kinesthetic coupling-formulation and experiment," *IEEE Transactions on Robotics and Automation. vol. 10, no. 5*, 1994.

[22] I. Aliaga, A. Rubio, and E. Sanchez, "Experimental quantitative comparison of different control architectures for master-slave teleoperation," *IEEE Transactions on Control Systems Technology*, 2004.

[23] M. Zhu and S. E. Salcudean, "Achieving transparency for teleoperator systems under position and rate control," *IEEE/RSJ International Conference on Intelligent Robots and Systems*, 1995.

[24] N. Stefanov, A. Peer, and M. Buss, "Role determination in human-human interaction," in *Third Joint Eurohaptics Conference and Symposium on Haptic Interfaces for Virtual Environment and Teleoperator Systems*, 2009.

[25] V. Hayward and K. E. Maclean, "Do it yourself haptics: part i," *IEEE Robotics Automation Magazine*, vol. 14, pp. 88–104, Dec 2007.

[26] A. Melendez-Calderon, L. Bagutti, B.Pedrono, and E.Burdet, "Hi5: a versatile dual-wrist device to study human-human interaction and bimanual control," *IEEE/RSJ International Conference on Intelligent Robots and Systems*, Sept. 2011.

[27] D. A. Lawrence and J. D. Chapel, "Performance trade-offs for hand controller design," in *Proceedings of the 1994 IEEE International Conference on Robotics and Automation*, pp. 3211–3216 vol.4, May 1994.

[28] L. B. Rosenberg and B. D. Adelstein, "Perceptual decomposition of virtual haptic surfaces," in *Proceedings of 1993 IEEE Research Properties in Virtual Reality Symposium*, pp. 46–53, Oct 1993.